



# IJPPR

INTERNATIONAL JOURNAL OF PHARMACY & PHARMACEUTICAL RESEARCH  
An official Publication of Human Journals

ISSN 2349-7203



Human Journals

**Research Article**

July 2016 Vol.:6, Issue:4

© All rights are reserved by Reda A. Mahmoud et al.

## Preparation and Characterization of Cytotoxic Drug-Loaded Gold Nanoparticles



**IJPPR**  
INTERNATIONAL JOURNAL OF PHARMACY & PHARMACEUTICAL RESEARCH  
An official Publication of Human Journals



ISSN 2349-7203

**Ahmed I. Mohamed<sup>1</sup>, Amal K. Hussain<sup>2</sup>, Gamal M. Zayed<sup>1</sup>, Shaykoon.M. Shaykoon<sup>3</sup>, Reda A. Mahmoud<sup>1\*</sup>**

<sup>1</sup>*Department of pharmaceuticals and industrial pharmacy, Faculty of pharmacy, University of Al-Azhar, Assiut branch, Egypt.*

<sup>2</sup>*Department of pharmaceuticals, Faculty of pharmacy, Minia University, Egypt.*

<sup>3</sup>*Department of pharmaceutical chemistry, Faculty of pharmacy, University of Al-Azhar, Assiut branch, Egypt.*

**Submission:** 10 July 2016  
**Accepted:** 15 July 2016  
**Published:** 25 July 2016

**Keywords:** Gold nanoparticles, tetrachloroauric acid, tri-sodium citrate, methotrexate, reduction method

### ABSTRACT

In the present study, we have conjugated methotrexate as a cytotoxic drug with gold nanoparticles modified with 11-mercaptoundecanoic acid to explore their potential application in cancer therapy. The anticancer activity of methotrexate-gold nanoparticle conjugates (GNP-MTX) was demonstrated in MCF-7 breast cancer cells. Gold nanoparticles have been synthesized using tri-sodium citrate as a reducing and stabilizing agent whereas 11-mercaptoundecanoic acid was used as a thiol functionalizing ligand in the aqueous medium. The formation of gold nanoparticles was confirmed from the characteristic surface Plasmon absorption band at 522 nm and the transmission electron microscopy revealed the average particle size to be (~ 20 nm). Methotrexate was conjugated to thiolated gold nanoparticles by using N-hydroxy succinimide (NHS) and N, N-Dicyclohexylcarbo-Di-imide (DCC) conjugation procedure and the binding was analyzed using Fourier transform infrared spectroscopy (FTIR) to investigate the possible chemical interaction between MTX and 11-mercaptoundecanoic acid.



HUMAN JOURNALS

[www.ijppr.humanjournals.com](http://www.ijppr.humanjournals.com)

## 1. INTRODUCTION

Cancer is considered as one of the horrible diseases. Despite the progression in the treatment of cancer, the cure rate for this horrible disease without any side effects is difficult to reach<sup>(1)</sup>. As surgery and radiation therapy may not always possible at advanced stages of cancer, chemotherapy is commonly preferred. Among various chemotherapeutic agents, methotrexate (MTX) is a preferable anti-metabolite drug. It is used in the treatment of certain cancers like breast, skin and lung cancer. As folate receptors are overexpressed on the surfaces of many cancer cells, MTX is one of the most commonly used chemotherapeutic agent for human malignancies<sup>(2)</sup>. However, most of the existing chemotherapeutic agents suffer from less selectivity, less solubility and shorter lifetime in blood stream in addition to the multi-drug resistance with the potential risk of side effects. Also, clinical studies have revealed that the curative effect of MTX regarding cancers was limited due to its toxic dose-related side effects and also due to the drug resistance of the tumor cells<sup>(3)</sup>. Based on these data, various targeted drug carriers have been developed to improve the existing therapeutic efficacy and also to protect the drug from biodegradation before reaching the target cells, as well as to reduce the expected side effects<sup>(4)</sup>. Furthermore, the nanoparticles mediated drug delivery systems (DDS) with diameter less than 30 nm may be preferred for enhanced permeability and retention effect (EPR) of tumors with reduced side effects<sup>(5, 6)</sup>. Various functionalized nanoparticles constituting a bio- conjugated assembly with anti-cancer drugs to formulate a targeted DDS have been reported<sup>(7)</sup>.

Considerable research efforts have been directed toward novel MTX delivery systems, such as nanoparticles<sup>(2, 8)</sup>, microspheres<sup>(9)</sup>, liposomes<sup>(10)</sup> and miscellaneous multiparticulate systems<sup>(11)</sup>. Among these, nanoparticles seem to be a promising tool for site specific delivery<sup>(12)</sup>, based on the fact that they will release the active pharmacological moiety in tumor cells owing to the enhanced permeability and retention (EPR) effect<sup>(13, 14)</sup>. Figure (1).

Methotrexate acts as anti-cancer drug through its anti-metabolic effect by Interfering with DNA and RNA growth by substituting for the normal building blocks of RNA and DNA<sup>(15)</sup>. There are a variety of nanoparticle systems currently being explored for cancer therapeutics<sup>(16)</sup>. The material properties of each nanoparticle system have been developed to enhance the delivery of drug to tumor, for example, hydrophilic surfaces can be used to provide the nanoparticles with the needed properties for longer circulation times and over positively charged surfaces can enhance endocytosis. The types of nanoparticles currently

used for cancer therapeutic applications include dendrimers<sup>(17)</sup>, liposomes<sup>(18)</sup>, polymeric nanoparticles<sup>(19)</sup>, micelles<sup>(20)</sup>, protein nanoparticles<sup>(21)</sup> and metallic nanoparticles<sup>(22)</sup>.

Gold nanoparticles (AuNPs) are particularly preferable because of their favorable properties such as non-toxicity<sup>(23)</sup>, ease of functionalization via ligand exchange which enhances the capability of binding with drug molecules<sup>(24)</sup> and simple fabrication in various sizes and shapes<sup>(25)</sup>.

Conventional techniques for aqueous synthesis of gold nanoparticles involve Turkevitch process of reduction of Au (III) Cl<sub>3</sub> with trisodium citrate. This process gives uniform and fairly spherical particles but proceeds at a very slow rate requiring nearly one hour for complete reduction of Au (III) Cl<sub>3</sub><sup>(24)</sup>.

To examine the cancer therapeutic effect of these nanoparticles, we have used 3-(4, 5-dimethylthiazol-2-yl)-2, 5-diphenyltetrazolium bromide (MTT) assay test. The obtained results proved that the MTX-AuNPs of small size (~20nm) exhibited considerably high toxic effects in breast cancer cell lines compared to the effects of equal doses of free MTX. These results suggest that anti-cancer drug-conjugated AuNPs have an enhanced and significant therapeutic effect.

## **2. MATERIALS AND METHODS**

### **2.1. Materials**

Methotrexate (C<sub>20</sub>H<sub>22</sub>N<sub>8</sub>O<sub>5</sub>) was obtained from Sandoz Pharmaceutical Company as freeze dried powder. Hydrogen tetrachloraurate trihydrate (HAuCl<sub>4</sub>.3H<sub>2</sub>O) was acquired from across organics, Belgium. Trisodium citrate dihydrate was provided from Fisher Scientific Company, USA. Mercapto Undecanoic Acid (MUA) was purchased from Sigma Aldrich, USA. N-hydroxy succinimide (NHS) and N, N-Dicyclohexylcarbo-Di-imide (DCC) were obtained from Sigma Aldrich, USA.

### **2.2. Preparation of gold nanoparticles**

The gold nanoparticles were prepared through reducing gold (III) ions with tri-sodium citrate by heating 100 ml distilled water until boiling under reflux, then we have used different concentrations of HAuCl<sub>4</sub>.3H<sub>2</sub>O and after 15 minutes, 1 ml of aqueous solution of tri-sodium citrate solution was added rapidly. Boiling and stirring were continued for 20 minutes. After

that, we removed the heating mantle and the solution was left with stirring till the solution was cooled down to reach room temperature. We have used different concentrations of citrate and gold solution to investigate the effect of citrate/gold ratio on the size of the nanoparticles. The produced nanoparticles were characterized by UV-Vis spectroscopy, size and zeta potential measurements<sup>(26)</sup>.

### **2.3. Preparation of MU-MTX conjugates**

In a typical experiment we added 1 mole of mercaptoundecanoic acid (MWT: 218.36) to dry di-methylformamide (DMF) then adding 2 moles of N-hydroxy succinimide (NHS) and 2 moles of N,N-Dicyclohexylcarbo-Di-imide (DCC) for the activation of the -COOH group. We have stirred this colloidal dispersion at room temperature for 6-8 hours, then adding 1.2 mole of methotrexate solution.

### **2.4. Characterization**

#### **2.4.1. UV-visible spectroscopy of the prepared nanoparticles**

Ultraviolet-visible light absorption spectra of the citrate-stabilized GNPs were taken at room temperature using a spectrophotometer (Schimadzu1601-double beam spectrophotometer, Shimadzu Company, Japan).

#### **2.4.2. Size measurement of nanoparticles by photon correlation spectroscopy (PCS)**

The size distribution and the zeta-potential of the prepared gold nanoparticles before and after polymer coating were analyzed by photon correlation spectroscopy PCS using Zetasizer ZSNano (Malvern instruments, UK).

#### **2.4.3. Nanoparticles morphological determinations using TEM imaging**

The morphology of the prepared gold nanoparticles was determined by TEM imaging. TEM samples were prepared by dropping gold colloids on carbon-coated copper grids followed by natural drying. The samples were observed on a JEM-100CXII transmission electron microscope (JEOL Ltd, Tokyo, Japan).

#### 2.4.4. IR analysis

The IR analysis was carried out using “Nicolet 6700 FT-IR instrument, Thermo-Fischer Scientific Corporation, Madison, USA” Department of Chemistry, Faculty of Science, Assiut University.

#### 2.5. Quantification

The amount of MTX-conjugated to AuNPs (% of loading) was quantified prior to the *in-vitro* study. Two calibration curves were applied individually for the MTX-AuNPs and the free MTX in the solution. In order to quantify the concentration of excess free MTX in the solution after the reaction, the calibration curve based on UV-Vis absorbance measurements of free MTX was constructed. The curve was constructed based on the absorption peak of pure MTX at 382 nm, the absorbance changes with the variation of the MTX solution concentration, the percentage (%) loading of MTX was estimated using equation (1):

$$\% \text{ loading} = (A-B) / B \times 100 \quad (1)$$

Where, A is absorbance of total MTX added to the GNP solution, and B is the absorbance of unbound MTX in the supernatant of the GNP-MTX solution after centrifugation.

#### 2.6. Cytotoxicity and viability assays

The JAR cell lines were cultured in DMEM/F12 supplemented with 10% fetal bovine serum and antibiotics at 37 °C with 5% CO<sub>2</sub>. Approximately 5000 cells (200 µL of a suspension of 2.5 × 10<sup>4</sup> cells/mL) were placed in each well of a 96-well culture plate kept for 24 h. For conducting cytotoxicity and viability experiments, serum-free medium was used to avoid the interference of the background absorption. The cancer cells in a serum-free medium were separately treated with reference AuNPs (naked GNPs), free MTX, and MTX-AuNPs. The concentrations of reference AuNPs and MTX-AuNPs were 100µg/ml. After gentle agitation, 100 µL of the culture medium was transferred into a new 96-well culture plate for the MTT assay, 25 µL of 5 mg/mL MTT was added into each well containing treated cells. After 4 hours, the supernatant was discarded and 100 µL of DMSO was added to each well. The mixture was shaken, and the optical density was measured at 570 nm using an ELISA reader scanning multi-well spectrophotometer (Perkin Elmer VICTOR 2, GMI, USA).

### 3. RESULTS AND DISCUSSION

#### 3.1. Preparation and characterization of gold nanoparticles

##### 3.1.1. Effect of citrate concentrations on the size of the produced nanoparticles

The size of the nanoparticles prepared by the reduction of gold salt normally depends on the type of reducing agent which determines the rate of nucleation and subsequently the particle growth. It was observed that the slow reduction produces large particles, while fast reduction usually produce smaller particles<sup>(27)</sup>. After addition of tri-sodium citrate to the boiled solution of the gold salt, a bluish color appeared indicating the formation of gold nuclei. A few minutes later, the solution was turned brilliant deep red due to the formation of the nanoparticles. The deep red color of gold nanoparticles in water is due to the strong light absorption in the visible region due to the oscillation of surface electrons after exposure to light. This phenomenon is characteristic for metallic nanoparticles called surface Plasmon resonance (SPR)<sup>(28)</sup>. Different concentrations of tri-sodium citrate were used. Through increasing the citrate to gold ratio from 10 to 30, the sizes of the particles were reduced from 35 nm to 22 nm. Table (1).

##### 3.1.2. UV-visible spectroscopy of the prepared nanoparticles

Particles synthesized by citrate reduction method can be obtained as monodisperse spheres where the sizes of which are controlled by the initial reagent concentrations and the chosen reaction conditions. The particles in aqueous dispersion are characterized by a deep red color with surface Plasmon resonance peak at about 524 nm as shown in Figure 2.<sup>(29)</sup>

##### 3.1.3. Size measurement of nanoparticles by photon correlation spectroscopy (PCS)

Many trials were conducted for the preparation of gold nanoparticles in different sizes by altering gold/citrate ratio. Thus, upon increasing the citrate concentration (citrate/gold=30) we have got gold nanoparticles with a small size and acceptable polydispersity (PDI) indices. So, we have considered these results are indicating for high reproducibility of the citrate reduction to prepare the gold nanoparticles. Figure shows the measured size distributions of different batches of the prepared GNPs. The obtained GNPs show a quite narrow monomodal size distribution with only one peak observed in the size distribution curve (Figure 3).

### 3.1.4. Nanoparticles morphological determinations using TEM imaging

TEM observations were employed to clarify the morphology of formed AuNPs. As seen from the TEM image of AuNPs, almost all of the AuNPs were spherical in shape and well dispersed. These results illustrated the formation of monodispersed and spherical AuNPs. Figure (2).

### 3.2. Investigation of MU-MTX conjugates by IR analysis

Firstly, it is so necessary to activate the carboxylic group of MUA to render it ready to form amide bond with the primary amine of MTX. Figure (3).

To understand the interaction between MTX and MUA, we carried out FTIR measurements. There is a strong peak is observed at  $1708\text{ cm}^{-1}$  due to the C=O stretch of tertiary amide (-CONH-). The weak broad peak around  $3361\text{ cm}^{-1}$  is assigned to tertiary amine group of MTX. The observed results clearly suggest that methotrexate is binding to MU-functionalized GNPs through the formation of an amide bond with the carboxyl group of MU as showed in Figure (6).

### 3.3. Cytotoxicity and viability assays

The *in-vitro* cytotoxicity characteristics of free MTX, naked GNPs and GNPs-MU-MTX against breast cancer cell lines (MCF-7) was determined by MTT assay. Regarding the *in-vitro* cytotoxicity assay, different concentrations of GNPs, free MTX and MTX loaded GNPs were used. The *in-vitro* cytotoxicity characteristics of them against a breast cancer cell line (MCF-7) was determined by MTT assay. Fig. 8 compares the cellular viability between free MTX, free GNPs and MTX loaded GNPs. From the data obtained from the figure (7), it was observed that at concentration above  $50\text{ }\mu\text{g/ml}$  of MTX-GNPs exhibited more cellular toxicity than that of naked gold nanoparticles. However, it was found that nanoparticles alone have also produced considerable cytotoxicity at concentration above  $80\text{ }\mu\text{g/ml}$ . From the *in-vitro* cytotoxic activity of drug, NPs and MTX-NPs, when the drug was conjugated with the nanoparticles, it was found that inhibitory concentration was decreased compared to the free MTX. The  $\text{IC}_{50}$  value for (MCF-7) cells was observed and it was found to be decreased from  $30.31\text{ }\mu\text{g/ml}$  for free MTX to  $9.41\text{ }\mu\text{g/ml}$  for MTX-NPs after 24 hours of incubation. Figure (4).



Methotrexate is a cytotoxic drug that works by interfering with DNA and RNA growth by substituting for the normal building blocks of RNA and DNA and is commonly used in the treatment of wide range of cancers<sup>(15)</sup>.

#### 4. CONCLUSION

In this work, we have demonstrated a proper method for direct synthesis of gold nanoparticles using (tri-sodium citrate reduction method), which gives us monodispersed and small sized gold nanoparticles (~ 20 nm), then making conjugation with methotrexate. From the *in-vitro* study (MTT assay) results, it was found that the methotrexate loaded gold nanoparticles showed enhanced cytotoxicity on a breast cancer cell line (MCF-7) in comparison to free methotrexate and free gold nanoparticles.

#### REFERENCES

1. Lv S, Li M, Tang Z, Song W, Sun H, Liu H, et al. Doxorubicin-loaded amphiphilic polypeptide-based nanoparticles as an efficient drug delivery system for cancer therapy. *Acta biomaterialia*, 2013, 9(12):9330-42.
2. Nogueira DR, Tavano L, Mitjans M, Pérez L, Infante MR, Vinardell MP. In vitro antitumor activity of methotrexate via pH-sensitive chitosan nanoparticles. *Biomaterials*, 2013, 34(11):2758-72.
3. Cho RC, Cole PD, Sohn K-J, Gaisano G, Croxford R, Kamen BA, et al. Effects of folate and folic acid on chemosensitivity of breast cancer cells. *Molecular cancer therapeutics*, 2007, 6(11):2909-20.
4. Brannon-Peppas L, Blanchette JO. Nanoparticle and targeted systems for cancer therapy. *Advanced drug delivery reviews*, 2004, 56(11):1649-59.
5. Coelho JF, Ferreira PC, Alves P, Cordeiro R, Fonseca AC, Góis JR, et al. Drug delivery systems: Advanced technologies potentially applicable in personalized treatments. *The EPMA journal*, 2010, 1(1):164-209.
6. Dai Y, Yang D, Kang X, Zhang X, Li C, Hou Z, et al. Doxorubicin conjugated NaYF<sub>4</sub>: Yb<sup>3+</sup>/Tm<sup>3+</sup> nanoparticles for therapy and sensing of drug delivery by luminescence resonance energy transfer. *Biomaterials*, 2012, 33(33):8704-13.
7. Chen J, Huang L, Lai H, Lu C, Fang M, Zhang Q, et al. Methotrexate-loaded PEGylated chitosan nanoparticles: synthesis, characterization, and in vitro and in vivo antitumoral activity. *Molecular pharmaceutics*, 2013, 11(7):2213-23.
8. Chen Y-H, Tsai C-Y, Huang P-Y, Chang M-Y, Cheng P-C, Chou C-H, et al. Methotrexate conjugated to gold nanoparticles inhibits tumor growth in a syngeneic lung tumor model. *Molecular pharmaceutics*, 2007, 4(5):713-22.
9. Liang LS, Jackson J, Min W, Risovic V, Wasan KM, Burt HM. Methotrexate loaded poly (l-lactic acid) microspheres for intra-articular delivery of methotrexate to the joint. *Journal of pharmaceutical sciences*, 2004, 93(4):943-56.
10. Kuznetsova NR, Sevrin C, Lespigneux D, Bovin NV, Vodovozova EL, Mészáros T, et al. Hemocompatibility of liposomes loaded with lipophilic prodrugs of methotrexate and melphalan in the lipid bilayer. *Journal of Controlled Release*, 2012, 160(2):394-400.
11. Kang H, Kim J-D, Han S-H, Chang I-S. Self-aggregates of poly (2-hydroxyethyl aspartamide) copolymers loaded with methotrexate by physical and chemical entrapments. *Journal of controlled release*, 2002, 81(1):135-44.
12. Khan ZA, Tripathi R, Mishra B. Methotrexate: a detailed review on drug delivery and clinical aspects. *Expert opinion on drug delivery*, 2012, 9(2):151-69.



13. Maeda H, Wu J, Sawa T, Matsumura Y, Hori K. Tumor vascular permeability and the EPR effect in macromolecular therapeutics: a review. *Journal of controlled release*, 2000, 65(1):271-84.
14. Matsumura Y, Maeda H. A new concept for macromolecular therapeutics in cancer chemotherapy: mechanism of tumoritropic accumulation of proteins and the antitumor agent smancs. *Cancer research*, 1986, 46(12 Part 1):6387-92.
15. Tanaka H, Matsushima H, Mizumoto N, Takashima A. Classification of chemotherapeutic agents based on their differential in vitro effects on dendritic cells. *Cancer research*, 2009, 69(17):6978-86.
16. Haley B, Frenkel E, editors. *Nanoparticles for drug delivery in cancer treatment. Urologic Oncology: Seminars and original investigations*; 2008: Elsevier.
17. Kukowska-Latallo JF, Candido KA, Cao Z, Nigavekar SS, Majoros IJ, Thomas TP, et al. Nanoparticle targeting of anticancer drug improves therapeutic response in animal model of human epithelial cancer. *Cancer research*, 2005, 65(12):5317-24.
18. Bellocq NC, Pun SH, Jensen GS, Davis ME. Transferrin-containing, cyclodextrin polymer-based particles for tumor-targeted gene delivery. *Bioconjugate chemistry*, 2003, 14(6):1122-32.
19. Betancourt T, Brown B, Brannon-Peppas L. Doxorubicin-loaded PLGA nanoparticles by nanoprecipitation: preparation, characterization and in vitro evaluation. 2007.
20. Sutton D, Nasongkla N, Blanco E, Gao J. Functionalized micellar systems for cancer targeted drug delivery. *Pharmaceutical research*, 2007, 24(6):1029-46.
21. Veronese FM, Pasut G. PEGylation, successful approach to drug delivery. *Drug discovery today*, 2005, 10(21):1451-8.
22. Lowery AR, Gobin AM, Day ES, Halas NJ, West JL. Immunonanoshells for targeted photothermal ablation of tumor cells. *International journal of nanomedicine*, 2006, 1(2):149.
23. Connor EE, Mwamuka J, Gole A, Murphy CJ, Wyatt MD. Gold nanoparticles are taken up by human cells but do not cause acute cytotoxicity. *Small*, 2005, 1(3):325-7.
24. Daniel M-C, Astruc D. Gold nanoparticles: assembly, supramolecular chemistry, quantum-size-related properties, and applications toward biology, catalysis, and nanotechnology. *Chemical reviews*, 2004, 104(1):293-346.
25. Palui G, Ray S, Banerjee A. Synthesis of multiple shaped gold nanoparticles using wet chemical method by different dendritic peptides at room temperature. *Journal of materials chemistry*, 2009, 19(21):3457-68.
26. Ji X, Song X, Li J, Bai Y, Yang W, Peng X. Size control of gold nanocrystals in citrate reduction: the third role of citrate. *Journal of the American Chemical Society*, 2007, 129(45):13939-48.
27. Azzam T, Eisenberg A. Monolayer-protected gold nanoparticles by the self-assembly of micellar poly(ethylene oxide)-b-poly( $\epsilon$ -caprolactone) block copolymer. *Langmuir*, 2007, 23(4):2126-32.
28. Wang G, Sun W. Optical limiting of gold nanoparticle aggregates induced by electrolytes. *The Journal of Physical Chemistry B*, 2006, 110(42):20901-5.
29. Kumar S, Gandhi K, Kumar R. Modeling of formation of gold nanoparticles by citrate method. *Industrial & engineering chemistry research*, 2007, 46(10):3128-36.

**Table (1): Effect of added amounts of sodium citrate on the size and the Surface Plasmon Resonance (SPR) of the synthesized gold nanoparticles**

HAuCl <sub>4</sub> . 3H <sub>2</sub> O (mg)	Tri-sodium citrate (mg)	gold/citrate ratio	Size (nm)	SPR maximum (nm)
5	50	1:10	35.14	525.5
5	100	1:20	27.17	524
5	175	1:30	22.19	523

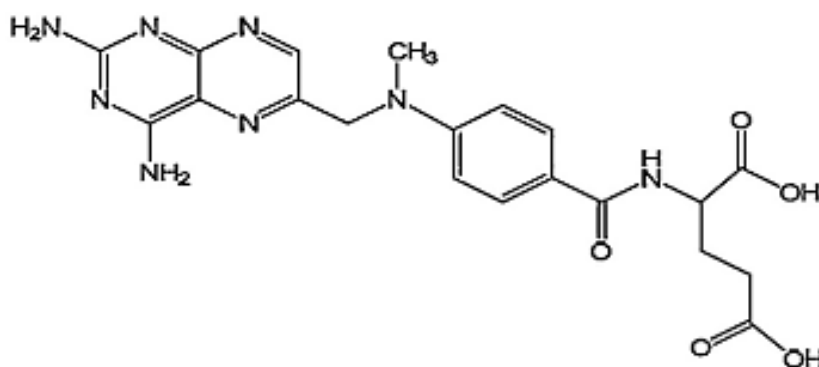


**Figure (1).Molecular structure of Methotrexate**

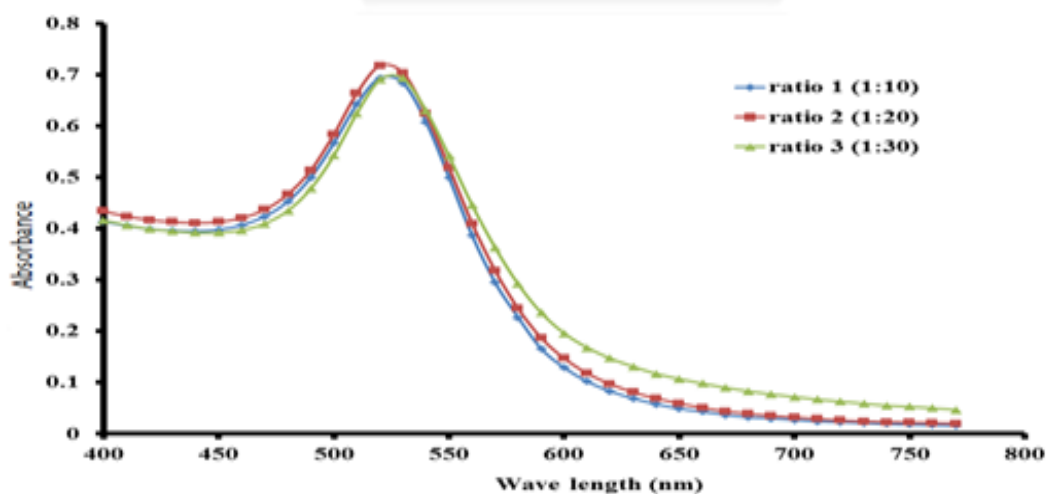


**Figure (2). UV-Vis absorption spectra of different gold nanoparticles preparations**

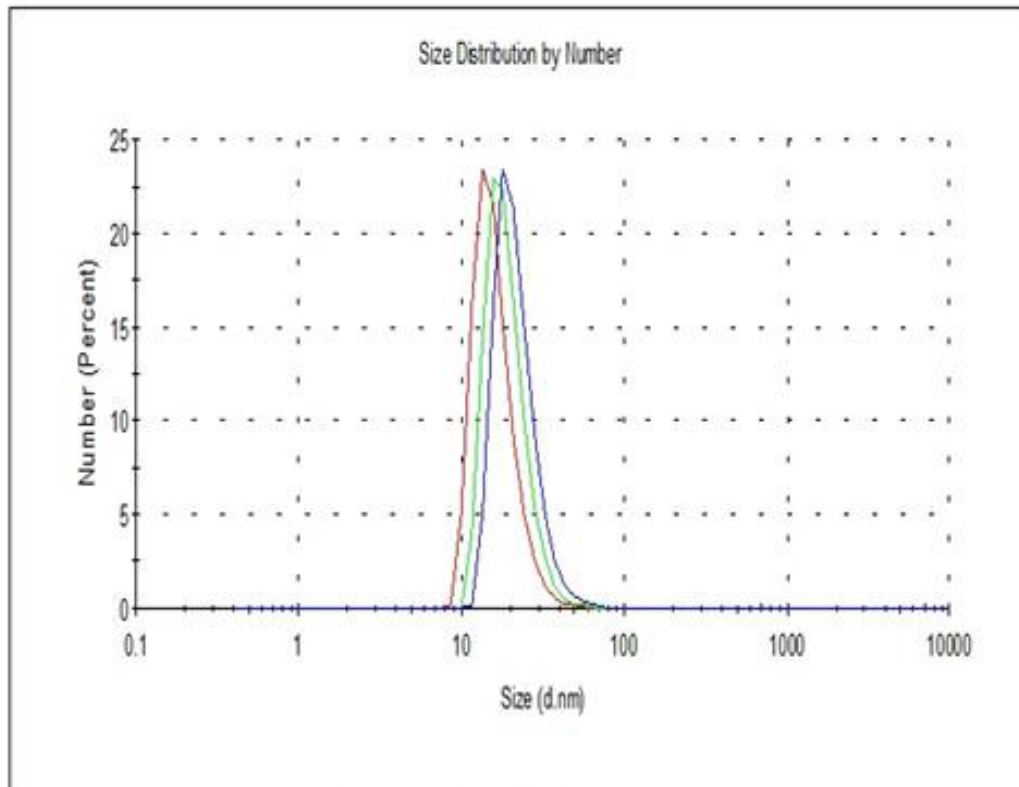


**Figure (3).Size distribution of different batches of synthesized gold nanoparticles**

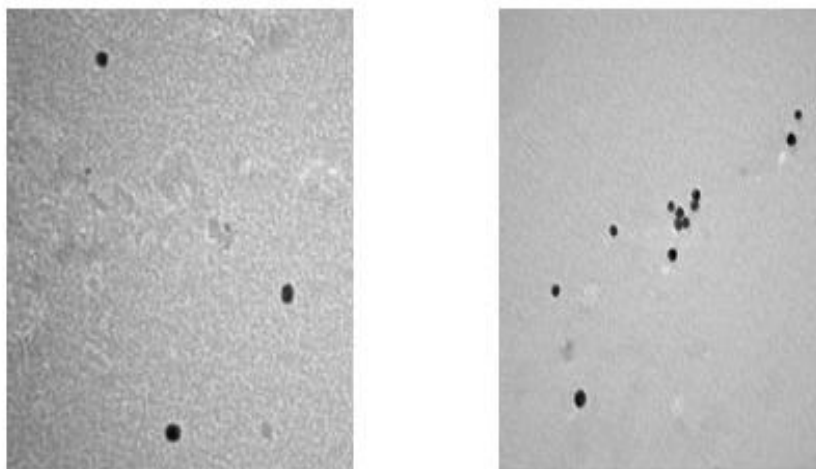


**Figure (4).TEM images of gold nanoparticles reduced by trisodium citrate method**

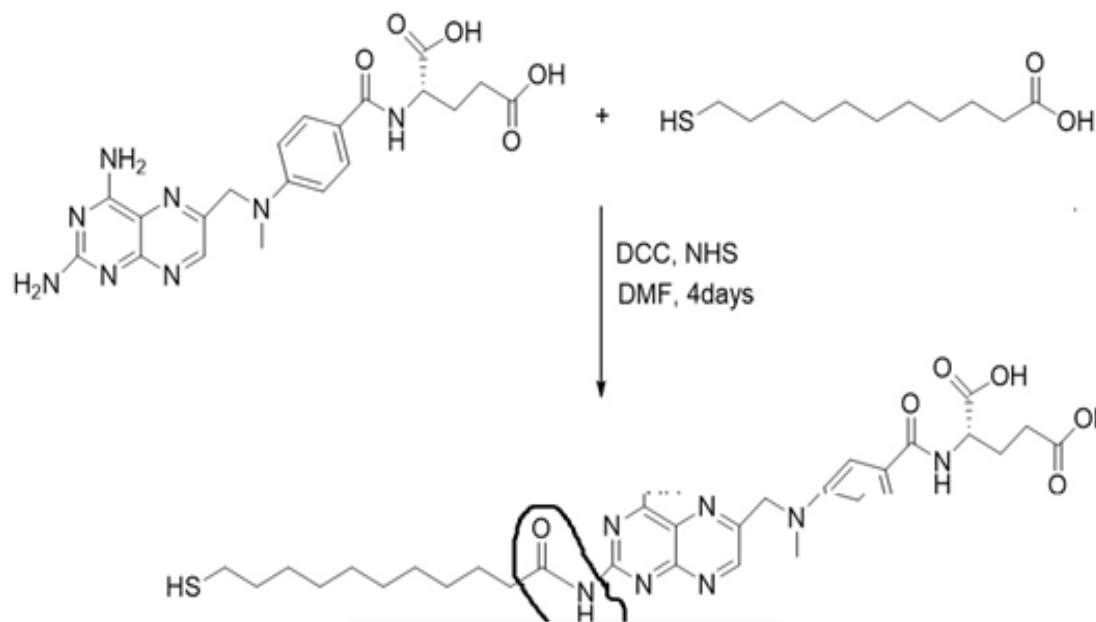


Figure (5). Conjugation between MTX and MUA

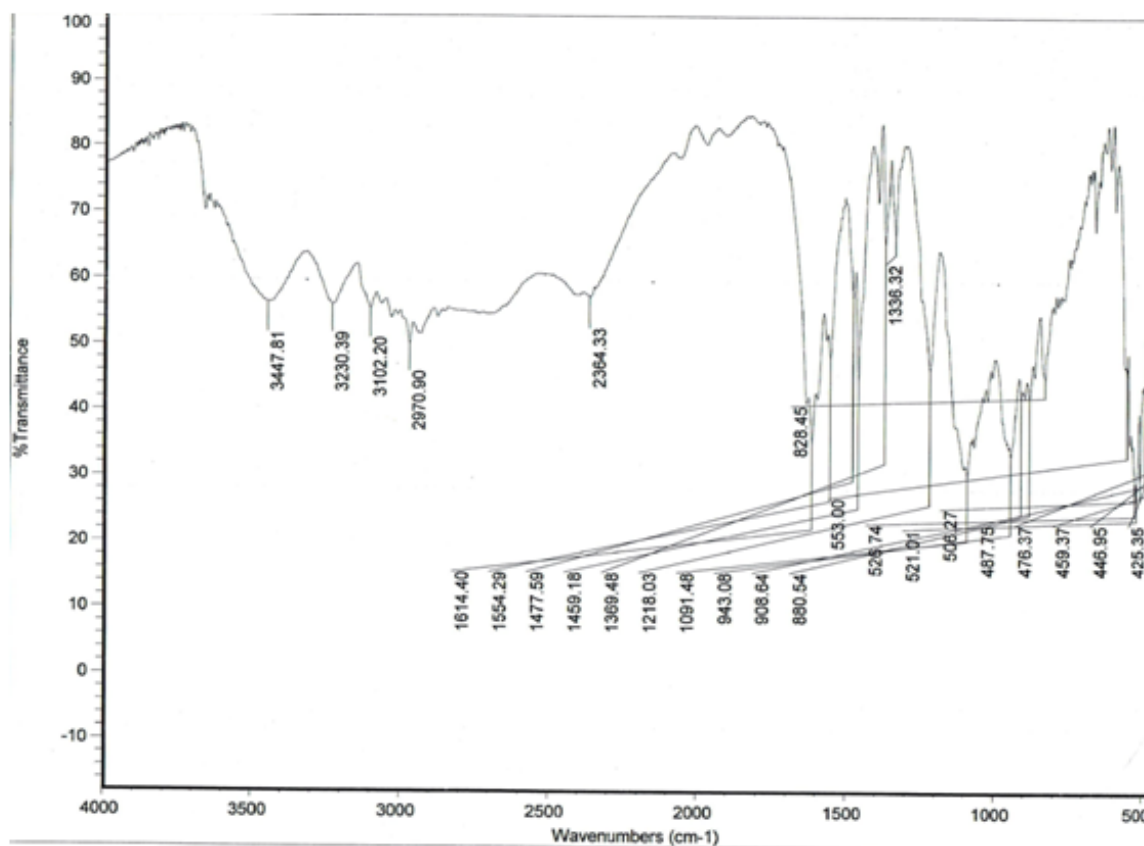
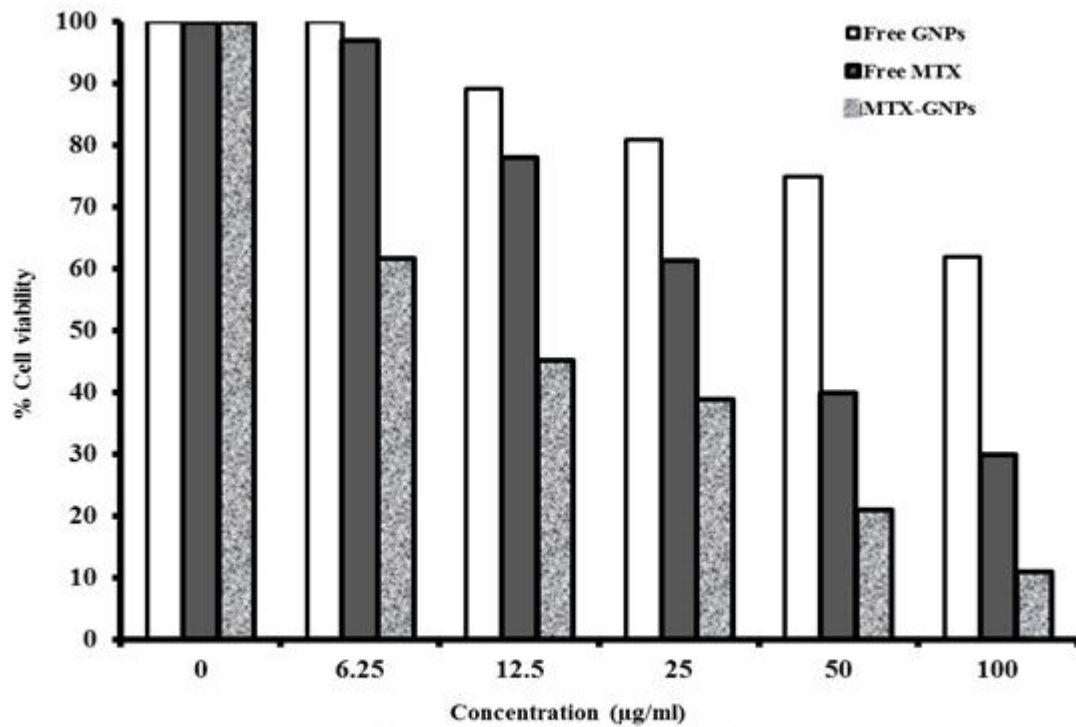


Figure (6). FTIR spectra of MTX and MU- MTX conjugates



**Figure (7):** The MTT assay showing the effect of naked GNPs, MTX and MTX loaded GNPs on breast cancer cell line.

HUMAN